Heliyon 9 (2023) e13008

Contents lists available at ScienceDirect

Heliyon

journal homepage: www.cell.com/heliyon

Research article

New iron(III) complexes with 2-formylpyridine thiosemicarbazones: Synthetic aspects, structural and spectral analyses and cytotoxicity screening against MCF-7 human cancer cells

Amany Fathy [a], Ahmed B.M. Ibrahim [b,*], S. Abd Elkhalik [a], Alexander Villinger [c], S.M. Abbas [a]

[a] Chemistry Department, Faculty of Science, Beni-Suef University, Beni-Suef 62521, Egypt
[b] Department of Chemistry, Faculty of Science, Assiut University, Assiut 71516, Egypt
[c] Institut für Chemie, Universität Rostock, Albert-Einstein-Str. 3a, 18059 Rostock, Germany

ARTICLE INFO

Keywords:
Tridentate ligands
Transition metals
Coordination compounds
X-ray diffraction
Cationic complexes
Anti-cancer activity

ABSTRACT

2-Formylpyridine thiosemicarbazone - iron (III) chelates $[FeL_2]Cl \bullet 2H_2O$ {$L = L^1$ (**C1**) [$\mathbf{HL^1}$ = 4-(4-Nitrophenyl)-1-((pyridin-2-yl)methylene)thiosemicarbazide] and $L = L^2$ (**C2**) [$\mathbf{HL^2}$ = 4-(2,5-Dimethoxyphenyl)-1-((pyridin-2-yl)methylene)thiosemicarbazide]} were prepared. The two ligand anions in each complex resulted in saturation of the iron coordination number and consequently the existence of these complexes as 1:1 electrolytes. As well, the iron in these complexes exhibits low-spin electronic configuration. X-ray crystallography of complex **C1** indicated its triclinic crystal system and P $\bar{1}$ space group. In addition, it proved the ligation through a thiol sulfur atom and two nitrogen atoms of pyridine and azomethine groups. This is while the presence of two water molecules of crystallization in the complex structure was also indicated. The ligand $\mathbf{HL^1}$ was selected for cytotoxicity screening against human MCF-7, A-549, HEPG-2 and HCT-116 cancer cells and the most enhanced activities were detected against the breast cells. Against these cells, the compounds $\mathbf{HL^1}$, $\mathbf{HL^2}$, **C1** and **C2** induced cytotoxicity, respectively, with IC_{50} values of 52.4, 145.4, 34.3 and 62.0 μM. However, against the healthy BHK cells, $\mathbf{HL^1}$ and $\mathbf{HL^2}$ caused cytotoxicity, respectively, with IC_{50} values of 54.8 and 110.6 μM and cytotoxicity with percent viabilities of 56.7 and 55.4% of the BHK cells by the complexes (137.4 μM of **C1** and 131.9 μM of **C2**) was determined. These activities against MCF-7 cells are less significant compared with the measured value for doxorubicin. But this standard is more toxic to normal cells than the thiosemicarbazones (IC_{50} (doxorubicin) = 9.66 μM against MCF-7 cells and 36.42 μM against BHK cells).

1. Introduction

Cancer is a fatal disease considered among the most important causes of mortality in the world that its development is based on a variety of factors including inactive lifestyle, stress, alcoholism, poor nutrition and genetic mutations [1]. Breast cancer, only after lung

* Corresponding author.
E-mail address: aibrahim@aun.edu.eg (A.B.M. Ibrahim).

https://doi.org/10.1016/j.heliyon.2023.e13008
Received 23 November 2022; Received in revised form 12 January 2023; Accepted 13 January 2023
Available online 24 January 2023

cancer as a reason of cancer related mortality, is extremely invasive and a prevalent cancer type with a great percentage of inflammation [2]. In 2021, the American Cancer Society estimated new cancer cases and related deaths of about 1,898,160 and 608,570 people in the United States and, among them, the numbers of breast cancer diagnostic cases and deaths are 284,200 and 44,130, respectively [3]. Iron is vital for human lives that assimilates with the heme "a major component in the cytochrome proteins myoglobin, leghemoglobin and hemoglobin mediating the redox processes of oxygen-carrying proteins" and is involved in the ATP generation, DNA synthesis and cell cycle progression [4]. Anemia is a clinical syndrome that results when the body possesses insufficient amount of iron for the metabolic demands, however consequences of insufficient iron produce compromised immunity in addition to physical impairment (e.g., lethargy and shortness of breath) and poor cognition [5]. In cancer cells, iron serves as a valuable nutrient to sustain fast proliferation and is also requested for the function of the enzyme ribonucleotide reductase that controls the rate determining step for the synthesis of DNA [6,7]. Hence, fighting many cancers can be via the development of specific chelators as a therapeutic avenue to remove iron from cells [8–10]. The iron chelating drug "bleomycin" functions to damage the cell DNA in the presence of dioxygen and hydrogen peroxide leading to lethality of the cancer cells [11]. Desferrioxamine (DFO), an approved therapeutic for the treatment of iron overload, has shown modest antitumor activity, but its usage in clinical trials is hampered by dose-limiting toxicity as well as unfavorable side effects [8,9]. Indeed, the iron chelators in both states, whether they bind iron or not, could benefit as therapeutics for fighting cancers. As ligands, iron chelators can demonstrate free iron deprivation in cancer cells significantly reducing the proliferation rate and influencing the cellular processes [12,13]. On the other hand, iron complexes experience redox cycling in cells leading to the production of reactive oxygen species, e.g. OH• radical, that induce cell injury, mitochondrial damage and DNA oxidation [14,15].

Thiosemicarbazones (TSCs) are significant metal chelators and their ability for iron chelation was proved [12]. These ligands, depending on diversity in their structures and various coordination modes, are significant for the multipurpose platforms for drug development strategies [16–28] as antimalarial [29], bactericidal [30], fungicidal [31,32], anticancer [33–35] and antitrypanosomal [36,37] agents. Indeed, compounds of N (4)-substituted heterocyclic TSCs with pyridine-2-carboxaldehyde that possess a system of tridentate N_2S atoms exhibit a niche cytotoxicity for inhibition of cellular proliferation [31–33] {e.g. triapine represents an anticancer drug for patients exhibiting advanced tumors [38–41]}. The action mechanism of these compounds is believed to be via disrupting the DNA biosynthesis by inhibiting the function of respective enzyme "ribonucleotide reductase" [40,41].

In abidance to previous research by us on TSC complexes [42–47] and anticancer chemotherapeutics [48,49], we here show preparation of two ferric iron complexes based on the ligands $\mathbf{HL^1}$ (4-(4-Nitrophenyl)-1-((pyridin-2-yl)methylene)thiosemicarbazide) and $\mathbf{HL^2}$ (4-(2,5-Dimethoxyphenyl)-1-((pyridin-2-yl)methylene)thiosemicarbazide). Further, we give details on a complex crystal structure in addition to the cytotoxic activities of both ligands and their complexes, relative to doxorubicin, against MCF-7 human breast cancer and baby hamster kidney (BHK) cell lines.

2. Experimental

2.1. Materials and instrumentation

Anhydrous ferric chloride alongside the chemicals (hydrazine hydrate, 4-nitrophenyl isothiocyanate, 2,5-dimethoxyphenyl isothiocyanate and pyridine-2-carboxaldehyde) and doxorubicin were involved in respective experiments as received from MERCK, Alfa Aesar or Sigma-Aldrich. The preparations and all manipulations during the experiments as well as the spectral and conductometric analyses were conducted in the air at ambient room temperature, unless mentioned else. The ligands {$\mathbf{HL^1}$ [50] and $\mathbf{HL^2}$ [45]} were obtained from the isothiocyanates according to respective literature each in two step experimental procedures. The first step includes the addition of hydrazine monohydrate to the isothiocyanates –N]C]S and this resulted in the breakage of the –N]C double bond and the formation of corresponding thiosemicarbazides {–NH–CS–NH–NH_2}. Second, the thiosemicarbazides were isolated by filtration, added to absolute ethanol containing drops of glacial acetic acid and allowed to react with pyridine2-carboxylaldehyde to form the thiosemicarbazone Schiff base ligands. Aqueous ethanol was used for crystallization of the thiosemicarbazones as high-purity ligands. The following CHNS data were determined for the ligands {Calcd. (Found) for $\mathbf{HL^1}$ (MW = 301.32 g/mol), C = 51.82 (51.71)%, H = 3.68 (3.66)%, N = 23.24 (23.41)% and S = 10.64 (10.67)%, and Calcd. (Found) for $\mathbf{HL^2}$ (MW = 316.38 g/mol), C = 56.94 (57.10)%, H = 5.10 (5.00)%, N = 17.71 (17.87)% and S = 10.13 (10.44)%}. The analyses for C, H, N and S in all ligands and complexes were via employing a Vario EL III instrument. The proton and carbon nuclear magnetic resonances of $\mathbf{HL^1}$ and $\mathbf{HL^2}$ were investigated utilizing a Bruker NMR spectrometer operating at 400 MHz, while tetramethylsilane (i.e. TMS) has been incorporated as the internal standard material. Electrical conductivities of the coordination compounds dissolved in dimethylformamide were elucidated with a conductivity meter "Jenway 4320". Vibrational spectral data of all compounds were carried out with an FT-IR spectrometer "Nicolet iS10" and the electronic spectral data in the 250–800 nm range were detected using a PerkinElmer Lambda 40 UV/VIS spectrometer. Effective magnetic moments for the complexes corrected for diamagnetism by Pascal constants [51] were calculated based on magnetic susceptibilities provided by a magnetic susceptibility balance "Sherwood MKI" employing the compound "Hg [$Co(SCN)_4$]" as a calibration reference.

2.2. Crystallographic analysis

Crystallographic analysis of **C1** was performed at 123 (2) K on a Bruker D8 QUEST diffractometer utilizing radiation of MoKα (λ = 0.71073 Å). The program package "Bruker SAINT" was used for the frame integration [52] and the absorption effects have been corrected with the Multi-Scan (SADABS) method [53]. The complex structure was determined with the help of "Bruker SHELXTL"

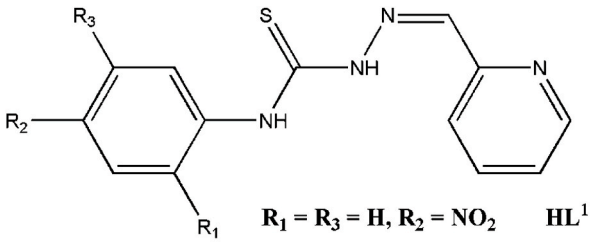

Fig. 1. General structure of the 2-formylpyridine thiosemicarbazone ligands.

software package for proper refinement [54]. Except for the hydrogen atoms, anisotropic refinement for the atoms was conducted. Hydrogen atom positions were calculated with a riding model. The N–bound H atoms were freely refined. The solved molecular graphic of complex **C1** was generated at 50% probability level with ORTEP-3 [55]. The data have been deposited with the Cambridge Crystallographic Data Centre (CCDC - 2175748) and can be obtained free of charge from: https://www.ccdc.cam.ac.uk/structures/.

2.3. Synthesis of the complexes

To the appropriate TSC ligand (100 mg: 0.332 mmol of $\mathbf{HL^1}$/0.316 mmol of $\mathbf{HL^2}$) in 10 mL of warm methanol, anhydrous ferric chloride (0.166 mmol (27 mg) to $\mathbf{HL^1}$ or 0.158 mmol (26 mg) to $\mathbf{HL^2}$) in 5 mL of methanol was added. After instant formation of dark brown solutions, room temperature stirring was continued for 60 min. The reaction mixtures were moved to a fridge for a month, then the solid products (single crystals of complex **C1**) were recovered by filtration, washed with small amount of methanol and diethyl ether and dried in ambient atmosphere.

$[Fe(L^1)_2]Cl\bullet 2H_2O$ **C1**: Yield = 65 mg (54%). Anal. Calcd. (Found) for $C_{26}H_{24}N_{10}O_6S_2FeCl$ (MW = 727.97 g/mol), C = 42.90 (42.60)%, H = 3.32 (3.33)%, N = 19.24 (18.98)% and S = 8.81 (8.66)%. FT-IR (KBr, cm^{-1}) = 3310 υ(^{4}NH), 1566 υ(C]N), 798 υ(CS), 1101 υ(N–N), 684 Py(iP) and 429 Py(OP). UV–Visible (DMSO, nm) = 262 and 394. Λ (DMF, $\Omega^{-1}cm^2mol^{-1}$) = 76.61. Effective magnetic moment (BM) = 2.44.

$[Fe(L^2)_2]Cl\bullet 2H_2O$ **C2**: Yield = 60 mg (50%). Anal. Calcd. (Found) for $C_{30}H_{34}N_8O_6S_2FeCl$ (MW = 758.07 g/mol), C = 47.53 (47.69)%, H = 4.52 (4.32)%, N = 14.78 (14.71)% and S = 8.46 (8.20)%. FT-IR (KBr, cm^{-1}) = 3387 υ(^{4}NH), 1529 υ(C]N), 814 υ(CS), 1098 υ(N–N), 641 Py(iP) and 454 Py(OP). UV–Visible (DMSO, nm) = 262, 292 and 396. Λ (DMF, $\Omega^{-1}cm^2mol^{-1}$) = 74.49. Effective magnetic moment (BM) = 2.34.

2.4. Antitumor activity studies

Human cancer cells of lung (A-549), liver (HEPG-2), breast (MCF-7) and colon (HCT-116) and healthy BHK cells were all provided from the American Tissue Culture Collection (ATCC). The cytotoxic activity studies of all compounds were performed thrice following the sulphorhodamine B (SRB) assay procedures [56]. The cells were planted in 200 μL of fresh medium in 96-well microtiter plates (about 4000 cells/plate) at 37 ºC and <5% of CO_2. After 24 h, the coordination and ligand compounds as well as doxorubicin (anticancer standard) were dissolved in dimethyl sulfoxide (DMSO) to form a series of solutions of each substance. Once the solutions were added to the cell plates, the plates were allowed to incubate in a CO_2 incubator for 48 h. Layering trichloroacetic acid (50%, 50 μL) at 4 °C on all plates resulted in fixing the cultures. The cultures were then washed with distilled water and stained for half an hour with SRB (0.4%, 50 μL) prepared in acetic acid (1%). The staining was in darkness at ambient temperature. Following rewashing with acetic acid (1%) and drying in air, tris(hydroxymethyl)aminomethane base (pH = 10.5, 10 mM, 200 μL) was added to liberate the dye. The dye concentration (consequently the cell viability) was determined in each plate by measuring the absorbance value at 570 nm with an ELISA microplate reader. Simultaneously with each experiment, the optical density in a control plate containing the same volume of DMSO instead of the sample solution was determined and this optical density was considered as percent viability of 100% of the cells. The IC_{50} values were calculated by GraphPad Prism 5.0 software [57].

3. Results and discussion

3.1. General aspects

The synthetic procedures of the ligands ($\mathbf{HL^1}$ [50] and $\mathbf{HL^2}$ [45]) (Fig. 1) are shown in much detail in the respective papers. The composition of both ligands was checked by CHNS microanalysis, FT-IR spectroscopy and ^{1}H and ^{13}C nuclear magnetic resonance spectroscopy. As dissolved in DMSO-d_6, the proton NMR spectral data of the ligands were investigated. $\mathbf{HL^1}$ cleared three singlet peaks in its spectrum seen at δ 8.62, 10.48 and 12.27 ppm and integrated each for the proton of the hydrazine N–H, thiourea N–H and azomethine N]CH– moieties, respectively. However, the detection of four doublet and two triplet peaks in the δ 7.43–8.40 ppm range is assignable for the ring protons in the ligand. Similarly, the ^{1}H NMR spectrum of ligand ($\mathbf{HL^2}$) possess five singlet peaks at δ 3.72, 3.85,

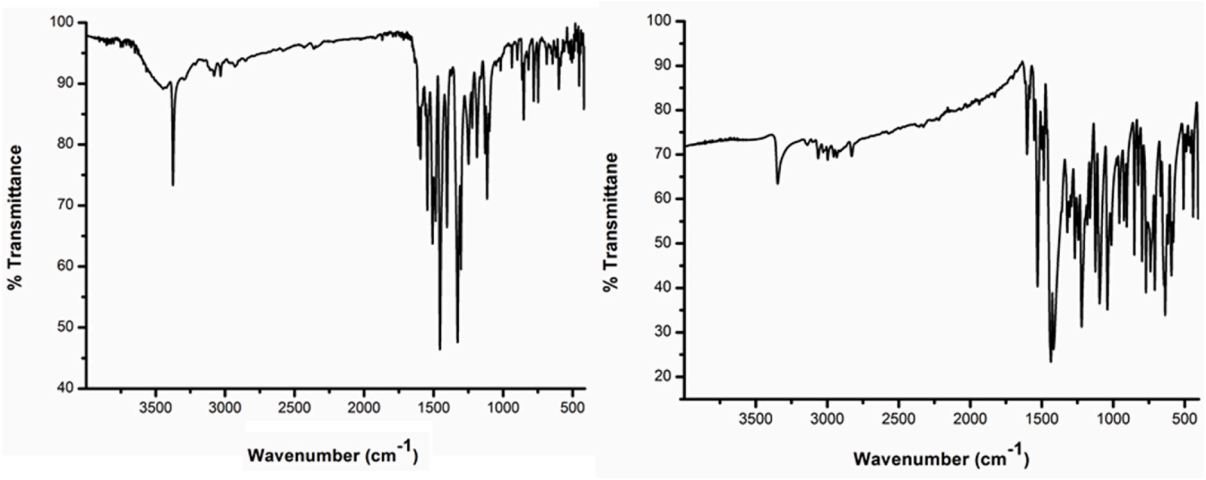

Fig. 2. FT-IR spectra of complexes **C1** (left) and **C2** (right).

8.21, 10.10 and 12.16 ppm (each of the first two peaks is integrated for three protons of one methoxy group, while the other three peaks are, respectively, assigned for the hydrazine N–H, thiourea N–H and azomethine N]CH– protons). In addition, seven peaks (one singlet, four doublet and two triplet) assigned for the ring protons in **HL^2** exist, in the δ 6.75–8.61 ppm range, in the ligand spectrum.

Upon addition of anhydrous ferric chloride to a methanolic solution of each ligand (mole ratio $FeCl_3$ 1:2 ligand), the transformation of the ligand solution color to dark brown was immediately observed. This color change indicated the complex formation, but indeed a long time (≈ one month in a fridge) was needed until the separation of the complexes in the solid form. These iron complexes were accessible in moderate yield of 50–54% and their analysis showed their perfect purity. The C, H, N and S compositional data suspected two ligand anions to satisfy the metal coordination number and a chloride gegenion to satisfy the trivalent oxidation state of iron {the act of pyridine-2-carboxaldehyde thiosemicarvazones as monoanionic tridentate ligands alongside their tautomeric thione – thiol behavior in their solutions was reported in several papers [42–47]}. In addition, it was suspected the existence of two water molecules and that was proved by X-ray crystallography for complex **C1** below. To check the 1:1 ionic nature of the complexes, molar conductivities of solutions of them (1 mM) in DMF were determined to be of 76.61 and 74.49 $\Omega^{-1}cm^2mol^{-1}$ in agreement with other 1:1 ionic complexes [58,59] and these conductivities exhibited no significant change after one day clearing high stability of the complexes in their DMF solutions [59]. Indeed, these iron complexes find great solubility in various types of organic solvents, i.e. polar aprotic (e.g. acetone, DMSO, DMF and acetonitrile) and protic (e.g. methanol) solvents and nonpolar solvents (e.g. chloroform). The effective magnetic moments of complexes **C1** and **C2** at room temperature were found of 2.44 and 2.34 B.M., respectively. These values agree with the value 2.33 B.M. reported for a similar complex and proved powerful strength of the TSC ligands that lead to the formation of low spin iron complexes with t_{2g}^5 electronic configuration [60].

The UV–Visible spectra of the ligands and complexes (10 μM) in DMSO were recorded. Indeed, each ligand displayed a single absorption at 333 nm (for **HL^1**) and 326 nm (for **HL^2**) related to n–π* transitions [61]. However, peaks at 262 and 394 nm for complex **C1** and others at 262, 292 and 396 nm for complex **C2** were detected. These peaks are ligand centered, except for those at 394 and 396 nm are due to S to Fe(III) charge transfer [62]. At higher concentrations, the d–d bands should appear, but tailing of the intense LMCT peaks at high concentrations obscured these peaks [63]. The FT-IR spectral analysis results of all compounds in potassium bromide pellets were recorded. Each ligand spectrum possessed two bands due to υ(^{2}NH) and υ(^{4}NH), respectively, at 3116 and 3292 cm^{-1} for **HL^1** and at 3136 and 3306 cm^{-1} for **HL^2** [43]. In the spectra of complexes **C1** and **C2** (Fig. 2), the first band is no longer observed due to coordination of the thiosemicarbazones with iron in their thiol form, while the second band was detected blueshifted due to different strength of hydrogen bonding in the complexes and their ligands [45]. Besides, there is also a band assignable for υ(CS) vibration in the spectrum of each ligand (at 846 cm^{-1} for **HL^1** and 842 cm^{-1} for **HL^2**) and the new location of these bands at lower wavenumbers, of 798 cm^{-1} for **C1** and 814 cm^{-1} for **C2**, after complexation proved bonding between iron and the TSC sulfur in both coordination compounds [42]. The coordination of iron with the azomethine nitrogen in the complexes could be proved by a peak related to stretching vibration in the azomethine moiety (this band appeared at 1582 cm^{-1} for **HL^1** and 1606 cm^{-1} for **HL^2** in the ligand spectra, but moved to the wavenumbers of 1566 and 1529 cm^{-1} for coordination compounds **C1** and **C2**, respectively) [45]. Moreover, the bands assigned for N–N bond stretching vibrations were shifted from the 1051–1078 cm^{-1} wavenumber range in the ligand spectra to the wavenumbers 1101 and 1098 cm^{-1} in the spectra of complexes **C1** and **C2**, respectively [46]. Finally the coordination of pyridine nitrogen is indicated by peaks due to in-plane and out-of-the plane ring deformation; these peaks for the complexes are located in the ranges of 641–684 cm^{-1} and 429-454 cm^{-1}, respectively, but the free ligand (**HL^1** and **HL^2**) spectra exhibited redshifts regarding both of the in-plane bands (664 and 622 cm^{-1}) and out-of-the-plane ones (404 and 407 cm^{-1}) [47].

Table 1
Crystallographic data and structure refinement parameters for [Fe $(L^1)_2$]Cl•$2H_2O$ (**C1**).

Empirical formula	$C_{26}H_{24}ClFeN_{10}O_6S_2$	μ (mm^{-1})	0.800
Formula weight	727.97	F(000)	746.0
Crystal system	Triclinic	θ range for data collection (°)	2.526 to 29.998
Space group	$P\bar{1}$	Reflections collected	45267
a (Å)	11.7976(15)	Unique refl. collected (R_{int})	8644 (0.0716)
b (Å)	12.4705(16)	Completeness to theta	99.8%
c (Å)	12.6005(16)	Parameters (Restraints)	511 (536)
α (°)	117.411(3)	Max. and min. transmission	0.746 and 0.670
β (°)	108.614(3)	GOF on F^2	1.030
γ (°)	96.315(4)	R_1 [I > 2σ(I)]	0.0448
Volume ($Å^3$)	1485.1(3)	w*R*2 (all data)	0.1253
Z	2	Largest diff. peak, hole/e $Å^{-3}$	0.798 and −0.640
Calculated density (g/cm^3)	1.628	CCDC number	2175748

Table 2
Selected bond distances, angles and hydrogen bonding parameters for [Fe $(L^1)_2$]Cl•$2H_2O$ (**C1**).

Atoms	Distance (Å)	Atoms	Angle (°)	Atoms	Angle (°)
Fe1–S1	2.2161(6)	S1–Fe1–S2	94.91(3)	Fe1–S2–C20	95.43(9)
Fe1–S2	2.2009(9)	S1–Fe1–N1	164.97(7)	Fe1–N1–C1	128.5(2)
Fe1–N1	1.995(2)	S1–Fe1–N2	84.26(7)	Fe1–N1–C5	112.3(2)
Fe1–N2	1.914(2)	S1–Fe1–N6	91.61(7)	Fe1–N2–N3	124.8(2)
Fe1–N6	2.000(3)	S1–Fe1–N7	96.20(7)	Fe1–N2–C6	117.6(2)
Fe1–N7	1.913(2)	S2–Fe1–N1	89.88(7)	Fe1–N7–N8	124.3(2)
S1–C7	1.751(3)	S2–Fe1–N2	94.28(7)	Fe1–N7–C19	117.9(2)
S2–C20	1.748(3)	S2–Fe1–N6	164.84(7)	Fe1–N6–C14	128.6(2)
N1–C1	1.331(3)	S2–Fe1–N7	84.95(7)	Fe1–N6–C18	112.7(2)
N1–C5	1.367(3)	N1–Fe1–N2	81.18(9)	C14–N6–C18	118.6(2)
N2–N3	1.371(3)	N1–Fe1–N6	87.27(9)	N8–N7–C19	117.9(2)
N2–C6	1.292(2)	N1–Fe1–N7	98.41(9)	C1–N1–C5	119.0(2)
N6–C14	1.330(3)	N2–Fe1–N6	99.98(9)	N3–N2–C6	117.6(2)
N6–C18	1.361(4)	N2–Fe1–N7	179.14(9)	N2–N3–C7	110.6(2)
N7–N8	1.379(3)	N6–Fe1–N7	80.75(9)	N7–N8–C20	110.5(2)
N7–C19	1.291(4)	Fe1–S1–C7	95.15(9)		
Hydrogen bonding interaction parameters					
D—H … A	d(D—H) Å	d(H … A) Å	d(D … A) Å	∠(D—H … A) °	Symmetry
N4–H4 ··· O5	0.88(4)	2.0195(4)	2.8902(8)	168.2(4)	–
N9–H9 ··· O6	0.87(5)	1.9978(4)	2.8368(4)	160.629(3)	–
O5–H5B ··· Cl1	0.82(5)	2.2407(4)	3.0486(7)	167.456(4)	–
O6–H6B ··· Cl1	0.82(3)	2.3641(3)	3.1818(3)	176.175(3)	–
C17–H17 ··· Cl1	0.950	2.7058(1)	3.6485(3)	171.824(2)	1-x, 1-y, 1-z
C4–H4 ··· Cl1	0.949	2.6726(1)	3.6193(3)	174.978(2)	1-x, 2-y, 1-z
O6–H6A … Cl1	0.82(3)	2.3379(3)	3.1520(3)	175.972(2)	1-x, 1-y, -z

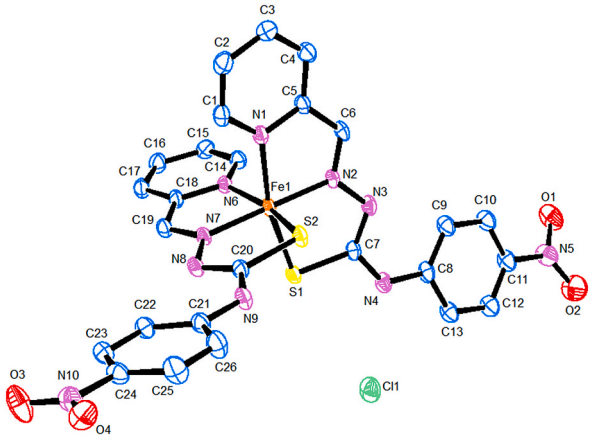

Fig. 3. ORTEP-III drawn molecular structure of [Fe $(L^1)_2$]Cl•$2H_2O$ (**C1**) with ellipsoids drawn with 50% probability level and all H atoms and H_2O molecules were removed for clarity.

Table 3
Antitumor screening results of various concentrations of **HL[1]** against percent viabilities of A-549, HEPG-2, HCT-116 and MCF-7 cells.

HL[1] (μM)	% Viability of cancer cells			
	A-549	MCF-7	HEPG-2	HCT-116
0.0	100	100	100	100
41.5	71.9	60.0	76.0	80.0
83.0	70.7	26.4	48.0	76.0
124.5	69.6	23.2	39.2	63.6
166.0	64.1	9.6	33.2	60.4

*Plates containing DMSO instead of the compound solution were used as control plates.

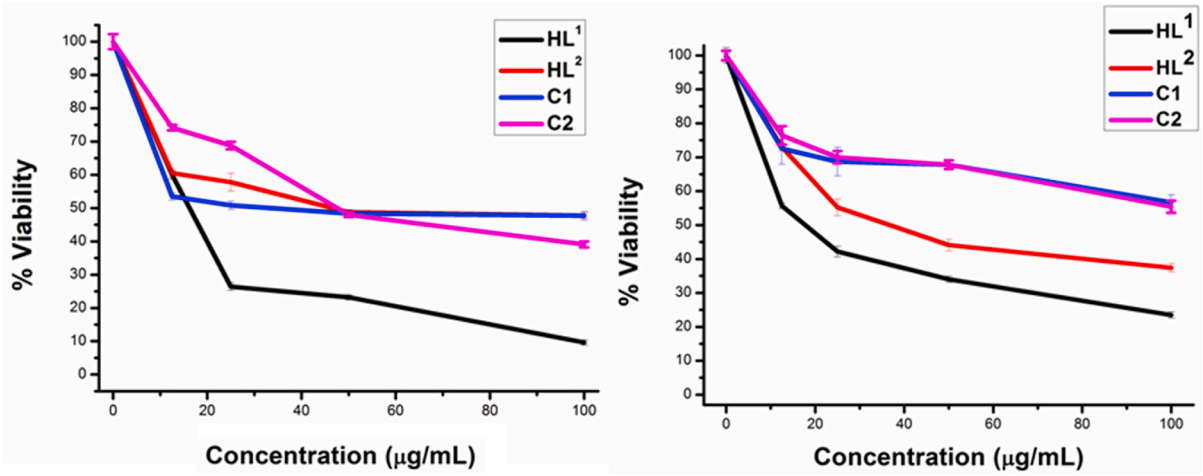

Fig. 4. Cytotoxic activities displayed by various concentrations of **HL[1]**, **HL[2]**, **C1** and **C2** against MCF-7 cancer (left) and BHK normal (right) cells.

3.2. Crystallographic studies on complex C1

A crystal of 0.12 × 0.12 × 0.17 mm of complex **C1** was selected for structural determination by X-ray crystallography that Table 1 summarizes crystal structure and refinement information for the complex, but Table 2 affords selected parameters for bonds, angles and possible H-bonds in the complex. Fig. 3 presents the molecular structure of **C1** that is composed of a ferric iron linked to a pair of TSC ligand monobasic anions alongside two non-coordinated water molecules (O5, O6) and a chloride ion (Cl1) present to compensate the remaining charge on the iron (III) ion. The two TSC ligand anions were seen wrapped around the iron (III) cation with almost orthogonal orientation to each other. These ligands exhibit N_2S tridentate anionic system through imine (N2, N7) and pyridine (N1, N6) nitrogen atoms and sulfur atoms (S1, S2) from the thiol moieties; all one ligand NNS atoms (i.e. N1, N2 and S1) and an imine nitrogen atom of the other TSC ligand (i.e. N7) form basal sites of an octahedron and the remaining atoms (i.e. N6 and S2) are in the axial positions. In the complex, the six coordination geometry around Fe(III) led to the involvement of iron in four five-membered chelate rings (Fe1–S1–C7–N3–N2, Fe1–N7–C19–C18–N6, Fe1–S2–C20–N8–N7 and Fe1–N1–C5–C6–N2). The two centroid-centroid distances for each couple of rings in the same ligand anion are 2.187 and 2.189 Å, and the distance of 1.633 Å between the two centroids of the NNS planes was investigated. Both of the imine nitrogen (N2 and N7) atoms in complex **C1** ligate the iron (III) ion in almost *trans*-manner {N2–Fe1–N7 angle = 179.14 (9)°}, but the pyridine (N1 and N6) and thiol (S1 and S2) donor atoms exist in *cis*-orientations {[N1–Fe1–N6] = 87.27 (9)° and [S1–Fe1–S2] = 94.91 (3)°}.

In a related literature, the crystal structures of iron complexes $[Fe(eT)_2]ClO_4$ and $[Fe(mT)_2]ClO_4$ {HmT = 2-Acetylpyridine-4-methyl-3-thiosemicarbazone and HeT = 2-Acetylpyridine-4-ethyl-3-thiosemicarbazone} were shown [64]. Comparing geometrical parameter in these complexes with those reported for complex **C1** revealed the following: Fe–S distances in **C1** are of 2.2009(9)–2.2161 (6) Å close to reported values {2.215(2)–2.223(2) Å} of similar angles in $[Fe(eT)_2]ClO_4$ and $[Fe(mT)_2]ClO_4$. Besides, Fe–N distances in **C1** range from 1.913(2) to 2.000(3) Å similar to values in the range of 1.914(4)–1.998(5) Å reported for $[Fe(eT)_2]ClO_4$ and $[Fe(mT)_2]ClO_4$ [64]. It is also noticeable that the Fe–N (pyridine) bonds (1.995(2) and 2.000(3) Å) in complex **C1** are longer compared to the complex Fe–N (imine) bonds (1.913(2) and 1.914(2) Å), while the Fe–N (pyridine) and Fe–N (imine) bonds in $[Fe(eT)_2]ClO_4$ and $[Fe(mT)_2]ClO_4$ fit, respectively, in the ranges of 1.982(5)–1.998(5) Å and 1.914(4)–1.924(2) Å [64]. Generally, the carbon—sulfur bonds in both TSC ligand anions {1.748(3) and 1.751(3) Å} are within reported values of C–S single bonds providing a strong proof for the act of the TSC ligands in the thiol form [64]. In addition, the C–N and N–N bond lengths in **C1** are of intermediate values between double and single bonds, because of charge delocalization along the ligand rings and chain [64].

The iron(III) complex (**C1**) in this research is packed mostly via intermolecular hydrogen bonds via the water molecules and the

Table 4
Half maximal inhibitory concentration (IC_{50} in μM) of ligands, complexes and doxorubicin against cancer MCF-7 and normal BHK cells.

Cell line	HL^1	HL^2	C1	C2	Doxorubicin
MCF-7	52.4	145.4	34.3	62.0	9.66
BHK	54.8	110.6	>137.4*	>131.9 *	36.42

IC_{50} values with (*) were not accurately determined, as the experiments were conducted up to the concentration of 100 μg/mL of each compound.

^{4}N–H moieties. This extensive net of hydrogen bonds stabilizes the complex structure that shows a distance of 6.5301(1) Å between the most neighboring iron centers.

3.3. Cytotoxicity screening against cancer cells

In this research, we selected the ligand **HL^1** (0–100 μg/mL) to perform an SRB assay screening experiment to explore which human cancer cells {A-549 (Lung), MCF-7 (Breast), HEPG-2 (Liver) and HCT-116 (Colon)} are more susceptible to our thiosemicarbazone compounds. As presented in Table 3, we reported the most significant results against MCF-7 cells due to the detection of the lowest percent viabilities of MCF-7 cancer cells in comparison to the other cells by the same concentrations of **HL^1**. Indeed, the IC_{50} values (the **HL^1** concentrations led to 50% cytotoxic activity) of 52.4 and 80.0 μM were, respectively, determined against the MCF-7 and HEPG-2 cells also evidencing the more activity of **HL^1** against the breast cancer cells. Nevertheless, it is interesting that the ligand **HL^1** demonstrated greater antitumor activity against HEPG-2 cells compared with several thiosemicarbazones [65] and hydrazones [66]. But it should be noted that complexes of ruthenium with nitrogen donor ligands demonstrated excellent antitumor cytotoxicity towards HEPG-2 cells with IC_{50} values of 18.0–22.3 μM (IC_{50} by cisplatin = 28.5 μM) [67].

Following this preliminary experiment, we explored the cytotoxic activity results of all compounds against the MCF-7 cells as model cells for the most globally prevalent women-related type of cancer (Fig. 4). Similarly to the screening experiment, solutions of each compound (0–100 μg/mL) were prepared in DMSO and the respective percent viabilities were recorded. Despite concentrations in μg/mL show information about required dosages of compounds to cause specific activities, these cannot afford reliable results regarding relative activities of compounds since similar dosages in μg/mL do not contain the same number of molecules of different compounds. Hence, we find necessity to compare with the molar concentrations of all compounds that resulted in 50% inhibition of the cancer cells.

For good comparison, we recorded IC_{50} values of 52.4, 145.4, 34.3 and 62.0 μM against the MCF-7 cells, respectively, afforded by **HL^1**, **HL^2**, **C1** and **C2** (Table 4). These values show clearly enhancing in the cytotoxic activities of the ligands via coordination with iron and complex **C1** gave the highest activity (lowest IC_{50}) against the MCF-7 cells. Despite the uptake of positively charged complexes by the cells is not expected to be as efficient as the uptake of neutral ligands at physiological pH [68,69], this considerable cytotoxicity of the iron complexes, compared with the ligands, may be correlated with profound activities known for other iron thiosemicarbazones. For example, an iron complex with triapine (3-aminopyridine-2-carboxaldehyde thiosemicarbazone) showed ascorbate oxidation, benzoate hydroxylation, glutathione depletion and DNA degradation in tumor cells [9]. As well, it was shown that this iron triapine complex is a more potent ribonucleotide reductase inhibitor compared with the ligand itself [70]. Since both of the complexes **C1** and **C2** contain two ligand anions, it is probably more adequate to compare our results with data generated for metal bisthiosemicarbazones. But the literature data on the bisthiosemicarbazone complexes are greatly varied with IC_{50} values spanning from more than 100 μM to less than 0.15 μM [71].

A comparison with the measured IC_{50} value of 9.66 μM for the reference drug doxorubicin against MCF-7 cells under the same experimental conditions indicated higher activity for the reference. It should be mentioned that we also evaluated the cytotoxic activities given by the compounds against healthy baby hamster kidney (BHK) cells (Fig. 4). Doxorubicin induced an IC_{50} value of 36.42 μM in BHK cells which indicates greater cytotoxicity of doxorubicin compared with the ligands **HL^1** (IC_{50} = 54.8 μM) and **HL^2** (IC_{50} = 110.6 μM). This is, but the cytotoxicity of the complexes is much less as percent viabilities of 56.7 and 55.4% of the BHK cells were determined for the complexes at their highest measured concentrations (i.e. 100 μg/mL: 137.4 μM of **C1** and 131.9 μM of **C2**). Therefore, based on these data on the cancer and normal cells, we conclude more suitability as anticancer agents for the complexes compared with the ligands. Further, doxorubicin showed greater activity against the cancer cells than the complexes, but the complexes appear to be much safer towards the normal cells than the standard.

4. Conclusion

This paper explains preparation of iron (III) complexes of thiosemicarbazone ligands with N_2S donor atom system. Analytics on these complexes explained their 1:1 electrolytic nature and low spin electronic configuration of iron in the complexes. In addition, the existence of octahedral geometry and two water molecules was confirmed by X-ray crystallography experiment on complex **C1**. The ligands' anticancer activities against breast MCF-7 cells were enhanced upon complexation. In addition, the complexes, compared with the ligands, have induced less toxicity towards BHK normal cells highlighting the importance of coordination in selective targeting of cancer. As a comparison, doxorubicin appears to be a more potent anticancer agent against MCF-7 cells, but much more toxic to the normal cells compared with the thiosemicarbazones.

Author contribution statement

Amany Fathy: Performed the experiments; Analyzed and interpreted the data.

Ahmed B.M. Ibrahim and S.M. Abbas: Conceived and designed the experiments; Contributed reagents, materials and analysis tools or data; wrote the paper.

S. Abd Elkhalik; Alexander Villinger: Contributed reagents, materials and analysis tools or data; Analyzed and interpreted the data.

References

[1] K. Kavithaa, M. Paulpandi, T. Ponraj, K. Murugan, S. Sumathi, Karbala, Int. J. Mod. Sci. 2 (2016) 46.
[2] P.Y. Liyanage, S.D. Hettiarachchi, Y. Zhou, A. Ouhtit, E.S. Seven, C.Y. Oztan, E. Celik, R.M. Leblanc, Biochim. Biophys. Acta, Rev. Cancer 1871 (2019) 419.
[3] R.L. Siegel, K.D. Miller, H.E. Fuchs, A. Jemal, Cancer statistics. CA: Cancer J. Clin. 71 (2021) 7.
[4] D.S. Kalinowski, D.R. Richardson, Pharmacol. Rev. 57 (2005) 547.
[5] I. Cavill, M. Auerbach, G.R. Bailie, P. Barrett-Lee, Y. Beguin, P. Kaltwasser, T. Littlewood, I.C. Macdougall, K. Wilson, Curr. Med. Res. Opin. 22 (2006) 731.
[6] A. Kicic, A.C.G. Chua, E. Baker, Anti Cancer Drug Des. 16 (2001) 195.
[7] E.D. Weinberg, Cancer Invest. 17 (1999) 507.
[8] Y. Yu, J. Wong, D.B. Lovejoy, D.S. Kalinowski, D.R. Richardson, Clin. Cancer Res. 12 (2006) 6876.
[9] T.B. Chaston, D.B. Lovejoy, R.N. Watts, D.R. Richardson, Clin. Cancer Res. 9 (2003) 402.
[10] D.R. Richardson, D.S. Kalinowski, S. Lau, P.J. Jansson, D.B. Lovejoy, Biochim. Biophys. Acta 1790 (2009) 702.
[11] S.T. Hoehn, H.D. Junker, R.C. Bunt, C.J. Turner, J. Stubbe, Biochemistry 40 (2001) 5894.
[12] Y. Yu, D.S. Kalinowski, Z. Kovacevic, A.R. Siafakas, P.J. Jansson, C. Stefani, D.B. Lovejoy, P.C. Sharpe, P.V. Bernhardt, D.R. Richardson, J. Med. Chem. 52 (2009) 5271.
[13] A. Mrozek-Wilczkiewicz, K. Malarz, M. Rejmund, J. Polanski, R. Musiol, Eur. J. Med. Chem. 171 (2019) 180.
[14] C. Stefani, G. Punnia-Moorthy, D.B. Lovejoy, P.J. Jansson, D.S. Kalinowski, P.C. Sharpe, P.V. Bernhardt, D.R. Richardson, J. Med. Chem. 54 (2011) 6936.
[15] T.B. Chaston, R.N. Watts, J. Yuan, D.R. Richardson, Clin. Cancer Res. 10 (2004) 7365.
[16] F.H. Allen, Acta Crystallogr. B58 (2002) 380.
[17] A.V. Kumar, Y. Sarala, S. Asha, S. Vanitha, S. Babu, A.V. Reddy, J. Appl. Pharmaceut. Sci. 84 (2018) 71.
[18] H.B. Shawish, M. Maah, S.N.A. Halim, S.A. Shaker, Arab. J. Chem. 9 (2016) 1935.
[19] P. Heffeter, V.F.S. Pape, E.A. Enyedy, B.K. Keppler, G. Szakacs, C.R. Kowol, Antioxidants Redox Signal. 30 (2019) 1062.
[20] R.R. Kumar, R. Ramesh, J.G. Małecki, J. Photochem. Photobiol. B Biol. 165 (2016) 310.
[21] C. Santini, M. Pellei, V. Gandin, M. Porchia, F. Tisato, C. Marzano, Chem. Rev. 114 (2014) 815.
[22] R. Jawaria, M. Hussain, H.B. Ahmad, M. Ashraf, S. Hussain, M.M. Naseer, M. Khalid, M.A. Hussain, M. Al-Rashida, M.N. Tahir, S. Asim, Inorg. Chim. Acta. Rev. 508 (2020), 119658.
[23] H. Pervez, N. Khan, J. Iqbal, S. Zaib, M. Yaqub, M.M. Naseer, Acta Chim. Slov. 65 (2018) 108.
[24] H. Pervez, N. Khan, J. Iqbal, S. Zaib, M. Yaqub, M.N. Tahir, M.M. Naseer, Heterocycl. Commun. 24 (2018) 51.
[25] H. Pervez, N. Khan, S. Zaib, M. Yaqub, M.M. Naseer, M.N. Tahir, J. Iqbal, Bioorg. Med. Chem. 25 (2017) 1022.
[26] K. Gaur, A.M. Vazquez-Salgado, G. Duran-Camacho, I. Dominguez-Martinez, J.A. Benjamín-Rivera, L. Fernández-Vega, L.C. Sarabia, A.C. García, M. Vega-Cartagena, S.A. Loza-Rosas, X.R. Acevedo, A.D. Tinoco, Inorganics 6 (2018) 126.
[27] M.E. Helsel, K.J. Franz, Dalton Trans. 44 (2015) 8760.
[28] E. Ramachandran, D.S. Raja, N.S.P. Bhuvanesh, K. Natarajan, Eur. J. Med. Chem. 64 (2013) 179.
[29] D.L. Klayman, J.F. Bartosevich, T.S. Griffin, C.J. Mason, J.P. Scovill, J. Med. Chem. 22 (1979) 855.
[30] J.G. Da Silva, L.S. Azzolini, S.M.S.V. Wardell, J.L. Wardell, H. Beraldo, Polyhedron 28 (2009) 2301.
[31] I.C. Mendes, J.P. Moreira, J.D. Ardisson, R.G. Dos Santos, P.R.O. Da Silva, I. Garcia, A. Castiñeiras, H. Beraldo, Eur. J. Med. Chem. 43 (2008) 1454.
[32] G.L. Parrilha, J.G. Da Silva, L.F. Gouveia, A.K. Gasparoto, R.P. Dias, W.R. Rocha, D.A. Santos, N.L. Speziali, H. Beraldo, Eur. J. Med. Chem. 46 (2011) 1473.
[33] D.C. Reis, M.C.X. Pinto, E.M. Souza-Fagundes, S.M.S.V. Wardell, J.L. Wardell, H. Beraldo, Eur. J. Med. Chem. 45 (2010) 3904.
[34] A.H. Pathan, A.K. Ramesh, R.P. Bakale, G.N. Naik, H.G.R. Kumar, C.S. Frampton, G.M.A. Rao, K.B. Gudasi, Inorg. Chim. Acta. 430 (2015) 216.
[35] I.C. Mendes, M.A. Soares, R.G. Dos Santos, C. Pinheiro, H. Beraldo, Eur. J. Med. Chem. 44 (2009) 1870.
[36] A. Merlino, D. Benitez, S. Chavez, J. Da Cunha, P. Hernandez, L.W. Tinoco, N.E. Campillo, J.A. Paez, H. Cerecetto, M. Gonzalez, Med. Chem. Commun. 1 (2010) 216.
[37] G.L. Parrilha, R.P. Dias, W.R. Rocha, I.C. Mendes, D. Benetez, J. Varela, H. Cerecetto, M. Gonzalez, C.M.L. Melo, J.K.A.L. Neves, V.R.A. Pereira, H. Beraldo, Polyhedron 31 (2012) 614.
[38] R.A. Finch, M.C. Liu, S.P. Grill, W.C. Rose, R. Loomis, K.M. Vasquez, Y.C. Cheng, A.C. Sartorelli, Biochem. Pharmacol. 59 (2000) 983.
[39] I. Gojo, M.L. Tidwell, J. Greer, N. Takebe, K. Seiter, M.F. Pochron, B. Johnson, M. Sznol, J.E. Karp, Leuk. Res. 31 (2007) 1165.
[40] S. Wadler, D. Makower, C. Clairmont, P. Lambert, K. Fehn, M. Sznol, J. Clin. Oncol. 22 (2004) 1553.
[41] J.E. Karp, F.J. Giles, I. Gojo, L. Morris, J. Greer, B. Johnson, M. Thein, M. Sznol, J. Low, Leuk. Res. 32 (2008) 71.
[42] A.B.M. Ibrahim, M.K. Farh, I.C. Santos, A. Paulo, Appl. Organomet. Chem. 33 (9) (2019) e5088.
[43] A.B.M. Ibrahim, M.K. Farh, S.A. El-Gyar, M.A. EL-Gahami, D.M. Fouad, F. Silva, I.C. Santos, A. Paulo, Inorg. Chem. Commun. 96 (2018) 194.
[44] G.A.-E. Mahmoud, A.B.M. Ibrahim, P. Mayer, J. Biol. Inorg. Chem. 25 (2020) 797.
[45] A.B.M. Ibrahim, M.K. Farh, P. Mayer, Inorg. Chem. Commun. 94 (2018) 127.
[46] A.B.M. Ibrahim, M.K. Farh, J.R. Plaisier, E.M. Shalaby, Future Med. Chem. 10 (21) (2018) 2507.
[47] A.B.M. Ibrahim, M.K. Farh, P. Mayer, Appl. Organomet. Chem. 33 (7) (2019), e4883.
[48] A.A.M. Aly, A.S.A. Zidan, A.B.M. Ibrahim, H.K. Mosbah, P. Mayer, S.H. Saber, J. Mol. Struct. 1249 (2022), 131634.
[49] A.A.M. Aly, A.B.M. Ibrahim, A.S.A. Zidan, H.K. Mosbah, S.A. Atta, I. Schicht, A. Villinger, J. Mol. Struct. 1256 (2022), 132508.
[50] V.F.S. Pape, S. Tóth, A. Füred, K. Szebényi, A. Lovrics, P. Szabó, M. Wiese, G. Szakács, Eur. J. Med. Chem. 117 (2016) 335.
[51] T.M. Salama, A.H. Ahmed, Z.M. El-Bahy, Microporous Mesoporous Mater. 89 (2006) 251.
[52] Bruker, SAINT, Bruker AXS Inc., Madison, Wisconsin, USA, 2012.
[53] G.M. Sheldrick, SADABS, University of Göttingen, Germany, 1996.
[54] G.M. Sheldrick, Acta Crystallogr. A71 (2015) 3.
[55] L.J. Farrugia, J. Appl. Crystallogr. 45 (2012) 849.
[56] P. Skehan, R. Storeng, D. Scudiero, A. Monks, J. McMahon, D. Vistica, J.T. Warren, H. Bokesch, S. Kenney, M.R. Boyd, J. Natl. Cancer Inst. 82 (1990) 1107.
[57] GraphPad Software, San Diego, California USA.
[58] W.J. Geary, Coord. Chem. Rev. 7 (1971) 81.
[59] N.R. Filipović, S. Bjelogrlić, G. Portalone, S. Pelliccia, R. Silvestri, O. Klisurić, M. Senćanski, D. Stanković, T.R. Todorović, C.D. Muller, Med. Chem. Commun. 7 (2016) 1604.
[60] A. Sreekanth, M.R.P. Kurup, Polyhedron 23 (2004) 969.
[61] A. Fathy, A.B.M. Ibrahim, S. Abd Elkhalik, A. Villinger, S.M. Abbas, Inorganics 10 (9) (2022) 145.
[62] A. Sreekanth, H.K. Fun, M.R.P. Kurup, J. Mol. Struct. 737 (2005) 61.

[63] M. Joseph, A. Sreekanth, V. Suni, M.R.P. Kurup, Spectrochim. Acta 64 (2006) 637.
[64] D.R. Richardson, D.S. Kalinowski, V. Richardson, P.C. Sharpe, D.B. Lovejoy, M. Islam, P.V. Bernhardt, J. Med. Chem. 52 (2009) 1459.
[65] M.H. Assaleh, S.K. Bjelogrlic, N. Prlainovic, I. Cvijetic, A. Bozic, I. Arandjelovic, D. Vukovic, A. Marinkovic, Arab. J. Chem. 15 (2022), 103532.
[66] D.S. Raja, N.S.P. Bhuvanesh, K. Natarajan, J. Biol. Inorg. Chem. 17 (2012) 223.
[67] G.-B. Jiang, W.-Y. Zhang, M. He, Y.-Y. Gu, L. Bai, Y.-J. Wang, Q.-Y. Yi, F. Du, J. Inorg. Biochem. 225 (2021), 111616.
[68] E.A. Enyedy, M.F. Primik, C.R. Kowol, V.B. Arion, T. Kiss, B.K. Keppler, Dalton Trans. 40 (2011) 5895.
[69] C.R. Kowol, R. Berger, R. Eichinger, A. Roller, M.A. Jakupec, P.P. Schmidt, V.B. Arion, B.K. Keppler, J. Med. Chem. 50 (2007) 1254.
[70] J. Shao, B. Zhou, A.J. Di Bilio, L. Zhu, T. Wang, C. Qi, J. Shih, Y. Yen, Mol. Cancer Therapeut. 5 (2006) 586.
[71] D. Palanimuthu, S.V. Shinde, K. Somasundaram, A.G. Samuelson, J. Med. Chem. 56 (3) (2013) 722.